ANALYTICAL APPROACHES FOR CALCULATION OF SHEAR STRESS ENHANCEMENT IN LAMINAR PULSED FLOWS

Celnik, M.S., Patel, M.J., Pore, M., Brahim[2], F., Augustin[2], W., Scholl, S.[2], Scott, D.M.[1] and Wilson, D.I.[1]

[1] Department of Chemical Engineering, New Museums Site, Pembroke St, Cambridge, CB2 3RA, UK
E-mail: diw11@cam.ac.uk
[2] Institute for Chemical and Thermal Process Engineering, Technical University of Braunschweig, Langer Kamp 7, 38106 Braunschweig, Germany

ABSTRACT

Analytical approaches have been developed for quantifying the enhancement of wall shear stress offered by intermittent flow pulsing, based on pressure gradient data, for the tubular and annular flow geometries commonly used in fouling and cleaning studies. The solutions are strictly only valid in the laminar regime. For the pipe geometry the two approaches, based on Fourier series integration and Green functions, respectively, both yielded results for non-regular pressure gradients in relatively short periods of computation time which were consistent with previously published solutions and CFD simulations. The Fourier series approach proved to be cumbersome for annular ducts so only the Green function approach was followed to completion.

The enhancement of surface shear stress over a baseline steady laminar flow is reported for both geometries: the enhancement depends on both the magnitude of the pressure gradient and the fraction of repeat period occupied by the pulse. The enhancement of shear stress in an annular flow geometry is also reported for the case of equivalent steady flow, where the total flow for the pulse and baseline remains constant. The improvement is small when long pulses are used.

A noteworthy observation is that the process conditions employed by Gillham and co-workers (2000) to enhance the cleaning of whey protein deposits during simulated alkaline cleaning-in-place tests were likely to have promoted turbulence in their system.

INTRODUCTION

Several experimental studies have demonstrated that the use of slow pulsed flows, *i.e.* the superposition of a pulse in velocity on a steady flow of liquid in the laminar or turbulent regime, can significantly increase the rate of cleaning (Gillham *et al*., 2000: alkaline cleaning of whey protein fouling deposits) or inhibit the deposition of particles or growth of crystalline fouling layers (Augustin and Bohnet, 2001: mineral scales in aqueous solutions). The effect is attributed to the periodic increase in shear stress imposed on the surface by the pulse. This mitigation route is attractive for viscous liquids, where the common practice of using turbulent flows in cleaning would be very

costly, or for systems where the inventory of liquid is to be minimised.

Flow pulsing can be achieved in practice using piston systems or gear pumps with appropriate valving: care needs to be taken to avoid water hammer and vibration in process equipment and control devices (*e.g.* valves). However, it should be noted that the pulsing need only be applied during part of a cleaning cycle, when the fouling deposit is soft enough to be removed by the enhanced shear.

A key engineering design parameter is the maximum shear stress imposed on the surface during the pulse cycle. This must be large enough to cause fracture or motion of the fouling layer (in cleaning) or inhibit attachment (in anti-fouling), the magnitude depending on the nature of the material and the surface, measured directly (*e.g.* Chew *et al*., 2005) or extracted from pilot plant test results where high flow velocities have been used to generate large shear stresses (or otherwise).

The effect of flow pulsing in pipes was reviewed by Edwards and Wilkinson (1971) and Çarpinlioğlu and Gündoğdu (2001). Most work in this area has focussed on the use of repeated sinusoidal flow pulses rather than less regular periodic profiles such as those reported by Augustin and Bohnet (1999), who imposed an isolated sinusoidal velocity pulse at regular intervals on a baseline steady flow. Their work showed significant mitigation effects on crystallisation fouling, particularly when the waviness of the flow, defined as the ratio of the maximum velocity of the flow pulse to the mean velocity of the steady flow, was ≥ 1 and flow reversal occurred near the wall, enhancing wall shear stresses. They supported their experimental studies, which featured steady flows in the turbulent regime, with computational fluid dynamics (CFD) studies which quantified the extent of flow reversal and shear stress enhancement.

In the laminar regime, pulsed flow also results in a deviation from the standard Poiseuille velocity profile. Harris *et al*. (1969) observed an 'annular effect' at high frequencies with regular sinusoidal pulsing which showed flow preferentially speeding up close to the wall. Edwards

and Wilkinson (1971) presented a model, based on the analytical solutions of Uchida (1956) and co-workers, which predicted these features. These models cannot be applied directly for non-sinusoidal pulsing, while quantification of shear stresses by CFD simulation is time and resource intensive.

The aim of this work was to develop analytically-based approaches to quantify the degree of shear stress enhancement which could be achieved in the laminar flow regime for a range of pulsation types. Two geometries are considered; pipe flow and flow along an annular duct. The latter is commonly employed in experimental investigations and also in industry where double-pipe heat exchangers are used to process viscous liquids, as they offer greater area for heat transfer than tubes and can be cleaned readily. The methodology is illustrated with simple pressure gradient profiles: the methodology is general and can be applied where the profile is known.

GOVERNING EQUATIONS

We consider flows consisting of a steady and a periodic component generated by the pressure gradient along the duct (pipe or annulus). The aim is to calculate the flow pattern generated by a particular pressure gradient as this can be readily measured in experiments. The main assumptions are

(i) The flow is incompressible and Newtonian.

(ii) The fluid is in the laminar flow regime.

(iii) The pressure gradient is axial only: $P = f(z)$.

(iv) The flow field is axially symmetric, therefore radial and azimuthal velocities are zero, and the system is three dimensional in r, z and t.

(v) Changes to the pressure gradient are effectively instantaneous in time, which is realistic for liquids in relatively short ducts.

(vi) The flow is fully developed and there are no entry effects.

(v) Constant physical properties.

Under the above assumptions the governing Navier-Stokes and continuity equations simplify to

$$\rho \frac{\partial u}{\partial t} - \frac{\mu}{r} \frac{\partial}{\partial r}\left(r \frac{\partial u}{\partial r}\right) = -\frac{\partial P}{\partial z}(t) \qquad [1]$$

which is a second order differential equation with two independent variables t and r. A key feature is that it is linear in the axial velocity $u(r,t)$ and is driven by a time

dependent axial pressure gradient, which can be written as the sum of the axial pressure gradient causing steady flow and that giving the pulsation. Pressure gradient is henceforth used to refer to the axial pressure gradient ($P' \equiv \partial P / \partial z$) rather than that with respect to time. Writing P' thus

$$P'(t) = P'_{ss} + P'_p(t) \qquad [2]$$

the velocity profile at a given point is given by the superposition of the solutions of the left hand side of [1] to each term in the pressure gradient in [2], namely

$$u(r,t) = u_{ss}(r) + u_p(r,t) \qquad [3]$$

The solutions for u_{ss} are well known, being

pipe
$$u_{ss}(r) = \frac{R^2}{4\mu}\left(-P'_{ss}\right)\left(1 - \left(\frac{r}{R}\right)^2\right) \qquad [4]$$

annulus
$$u_{ss}(r) = \frac{R^2}{4\mu}\left(-P'_{ss}\right)\left(b^2 - a^2 + \frac{b^2 - a^2}{ln[b/a]}\cdot ln\left(\frac{r}{b}\right)\right) \qquad [5]$$

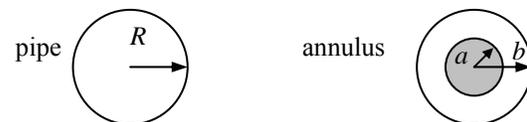with the geometry depicted in Figure 1.

Figure 1 Definition of geometries

Two approaches have been developed to generate the velocity profile and consequently the wall shear stress behaviour for a general pressure gradient profile: a Fourier Series method, similar to that employed by Edwards and Wilkinson for sinusoidal pulsation, and a new Green function approach.

I. Fourier Series Solutions

Practical applications of flow pulsing are unlikely to feature perfect periodic functions such as sine waves, and, further, intermittent pulses such as those used by Augustin and Bohnet demonstrated that continuous pulsing was not required for fouling mitigation, thereby saving energy. Gillham's experiments on cleaning-in-place of whey protein deposits in aqueous sodium hydroxide featured intermittent pulses introduced by bellows and piston arrangements: the pressure profiles measured at the entry to the tube test sections can be approximated by the intermittent triangular functions as shown in Figure 2.
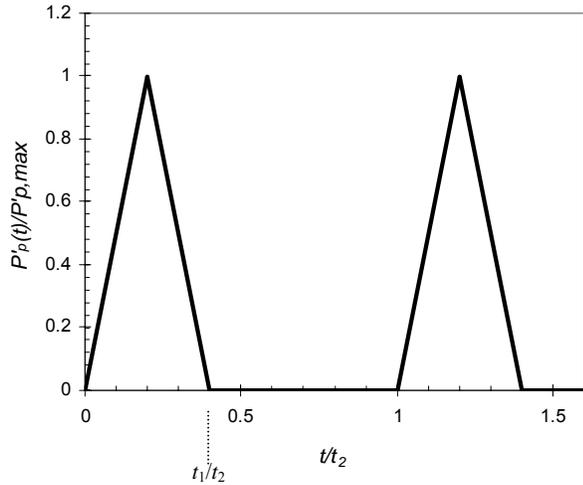
Figure 2 Idealised pressure gradient pulse profile, plotted as ratio of $P'_p(t)/P'_{p,max}$ with period t_2. Triangular pulse length t_1.

In the Fourier series approach, we exploit the property that profiles such as those in Figure 2 can be approximated as a Fourier series of N harmonic terms. The overall response is then the sum of the responses to the individual frequency terms, weighted according to their contribution to the series by the coefficients a_i and b_i.

$$u(r,t) = u_{ss}(r) + u_0(r) + \sum_{n=1}^{N} u_n(r,t)_{cos} + \sum_{n=1}^{N} u_n(r,t)_{sin} \quad [4]$$

The solutions for the tubular geometry are (see Edwards and Wilkinson, 1971)

$$u_n(r,t)_{cos} = \mathrm{Re}\left[\frac{a_n}{i\omega\rho}\left\{1 - \frac{J_0\left[\lambda_n \beta i^{1.5}\right]}{J_0\left[\lambda_n i^{1.5}\right]}\right\} exp(in\omega t)\right] \quad [5]$$

$$u_n(r,t)_{sin} = \mathrm{Im}\left[\frac{b_n}{i\omega\rho}\left\{1 - \frac{J_0\left[\lambda_n \beta i^{1.5}\right]}{J_0\left[\lambda_n i^{1.5}\right]}\right\} exp(in\omega t)\right] \quad [6]$$

with $\lambda_n = R\sqrt{\dfrac{n\omega\rho}{\mu}}$ \quad [7]

and where J_0 is a Bessel function of zero order. The shear stress at the wall is obtained from equation [4],

$$\tau_w = -\mu\left(\frac{\partial u(r,t)}{\partial r}\right)_{r=R} \quad [8]$$

and this requires manipulation of the complex parts of [5] and [6]. This was achieved by introducing Kelvin functions $ber(x)$ and $bei(x)$, where

$$ber(x) = \mathrm{Re}\left\{J_0\left(xi^{1.5}\right)\right\} \quad [9]$$

$$bei(x) = \mathrm{Im}\left\{J_0\left(xi^{1.5}\right)\right\} \quad [10]$$

re-writing [4] in terms of ber and bei, and differentiating the functions using the polynomial approximations given in Abramowitz and Stegun (1967). A detailed description of the Fourier series approach is given in Patel and Pore (2003). Celnik (2004) considered the analogous treatment for the annular geometry and concluded that the solutions were cumbersome and offered no advantage over the Green function approach.

II. Green function approach

Equation [1] is a linear partial differential equation with a driving term on the RHS (the pressure gradient) which is a function of time, $f(t)$. Writing the LHS in terms of an operator on u, L, gives

$$L \cdot u = f(t) \quad [11]$$

Let a function $G(r, t)$ exist such that

$$L \cdot G(r, t - t') = \delta(t - t') \quad [12]$$

where δ is the Dirac delta function: this Green function G is the solution of the original differential equation for a delta impulse in pressure gradient, $f(t) = \delta(t)$. One can then write

$$f(t) = L \cdot \left[\int_{-\infty}^{t} G(r, t - t') f(t') dt'\right] \quad [12]$$

and the velocity is given by

$$u(r,t) = \int_{-\infty}^{t} G(r, t - t') f(t') dt' \quad [13]$$

It is important to note that no assumption has been made concerning the form of $f(t)$ and therefore this method can be applied to any pressure gradient as long as the Green function can be identified. The Green function for velocity for laminar pipe flow is

$$G_{vel}(r,t) = \frac{2}{\rho} \sum_{n=1}^{\infty} \frac{J_0\left(\Lambda_n \frac{r}{R}\right)}{\Lambda_n J_1(\Lambda_n)} exp\left(-\frac{\mu\Lambda_n^2}{\rho R^2} t\right) \quad [14]$$

where Λ_n is the nth zero of J_0 (zeroth order Bessel function of the first kind) and J_1 is a first order Bessel function of the first kind. Similar expressions were obtained for shear stress and total flow rate. When integrated, *i.e.* evaluating [13], the calculation gives an indication of the transient response of the system which should approach the steady state result calculated directly by the Fourier Series method.

III. Annular geometry

As noted above, the annular geometry proved to be cumbersome in the Fourier series approach when calculating the shear stress at either wall, so the Green function method has been used alone. The form of *G* for the annulus has been derived by Celnik (2004) and differs from the pipe case but the methodology is similar. It should be noted that Green function approach describes a transient which eventually reaches steady state. As part of this work on annular systems, a novel methodology was developed which allowed the steady state behaviour to be calculated directly. A detailed description is given in Celnik *et al.* (2005).

CALCULATION

All analytical and semi-analytical calculations were performed using *Mathematica*™ versions 4.2 and 5 (Wolfram Research) on a standard PC or laptop. Two geometrical cases were considered, of particular interest. The first was a simple tube, representing the test section used by Gillham *et al.* (2000) with NaOH at 50 ºC, where the parameters were $R = 3.05$ mm, $\mu = 0.547$ mPa s and $\rho = 988$ kg/m^3. The second case was an annular section representing the laboratory device at Braunschweig featured in the accompanying paper by Bode *et al.* (2005). This featured dimensions $a = 7.5$ mm and $b = 12.5$ mm, with solution properties those of water at 20 ºC.

The results for pulsation in pipe flows were compared with computational fluid dynamics simulations generated using Fluent™ on a standard PC. Here, the flow along a 0.5 m pipe was simulated with time steps of 0.001 s in order to calculate the fully developed velocity profile. The version of Fluent used required the pressure gradient to be entered as input and could return the velocity profile and pressure profile through the system. These were then compared with the Mathematica predictions.

An important criterion in all these calculations is the threshold for the onset of turbulence in pulsating flows. Discussions of this criterion (*e.g.* Çarpinlioğlu and

Gündoğdu, 2001; Çarpinlioğlu, 2003) do not mention annular systems or non-sinusoidal pressure gradients. Experimental studies such as that by Donovan *et al.* (1994) reported no significant indications of turbulence below a maximum Reynolds number of 2000 during experiments with water for a sinusoidal pressure gradient profile over a broad range of amplitudes, and this value has been used here to provide a confidence limit on the accuracy of the calculations.

RESULTS AND DISCUSSION

Verification studies

Harris *et al.* (1969) generated sinusoidal oscillatory flows (*i.e.* $P'_s=0$) in a circular tube of diameter 25.2 mm using two cams of different eccentricities contacting a plate at one end of the tube. The liquid density was 1057 kg m^{-3} and viscosity 0.0552 Pa s. Small polystyrene spheres of density 1055 kg m^{-3} were mixed with the flow, each of which left a visible, measurable track in the fluid as it travelled axially back and forth during the oscillations. The length of these tracks was the distance travelled by the particle during half of the period of oscillation t_2, as during the other half of the period of oscillation the particle travelled in the opposite direction along the track already made in the fluid during the first half. An analytical prediction $S(r)$ for the track lengths is

$$S(r) = \int_0^{0.5t_2} u(r,t)dt \qquad [15]$$

and relied on the particles being neutrally buoyant and small and thus acting as elements of fluid. Harris *et al.* reported results for flows driven at 1, 2, 5 and 7 Hz. Due to the experimental set up, the controlled or input parameter was a sinusoidal volumetric flow rate and the amplitudes of the oscillatory pressure gradients were not reported. However, this should not affect the shape of the velocity profile as long as the system remains laminar. Figure 3 shows a comparison of their results and the radial track lengths calculated using the Fourier series approach. The agreement is excellent.
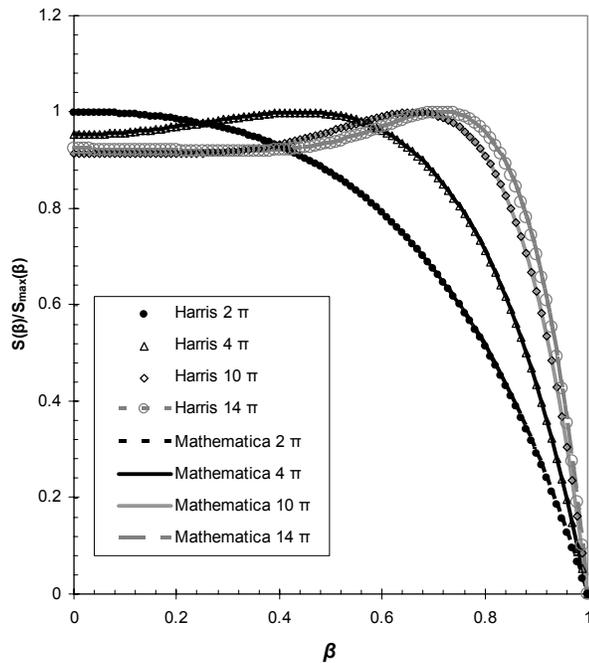
Figure 3 Comparison of Harris *et al.* (1969) results for variation of track length S with radial position $\beta = r/R$, and those predicted here using Mathematica™. Values in legend indicate the frequency of the sinusoidal oscillation.

An intermittent pulse profile similar to Figure 2 was used to compare the model predictions with CFD results obtained using Fluent. The form in Figure 2 was chosen to mimic the pressure profile reported by Gillham *et al.* (2000), for which the parameters were estimated to be P'_p = 49950 Pa/m, P'_{ss} = 50 Pa/m, t_1 = 0.02s and t_2 = 5.0 s. However, both approaches indicated that the maximum Reynolds number during this cycle reached 70,000, which clearly breached the laminar transition threshold, even though the steady flow Reynolds number was low. This result indicates that the effectiveness of the pulsing regime used by Gillham and co-workers lay in the generation of turbulence. It was also unlikely that the velocity profile would have returned to steady state within the period.
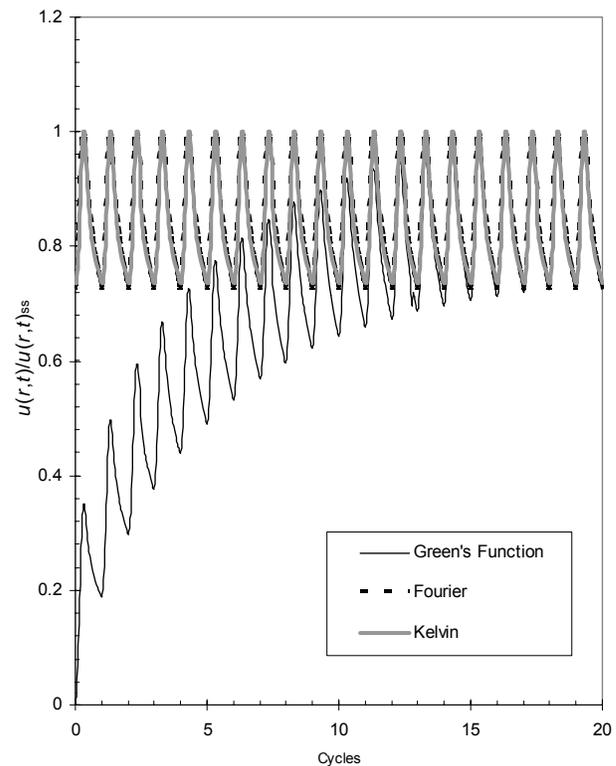

Figure 4 Comparison of predicted velocity at an arbitrary radial co-ordinate for the different analytical approaches, for a pressure pulse of the form of Figure 2 in a pipe.

Comparisons with Fluent were therefore performed with smaller pressure gradients (P'_p = 483× P'_{ss}) and a longer period, t_2 = 8 s, which gave a maximum Reynolds number of 1830. The small value of t_1/t_2 required a large number of terms in the Fourier series and 2000 were used here. Figure 4 shows a sample of velocity transients generated by the two semi-analytical approaches, where the Kelvin function set refer to the alternative representation of the velocity profiles in terms of *ber* and *bei*. The transient behaviour of the Green function approach is immediately evident and converges to the steady state result within 20 cycles.
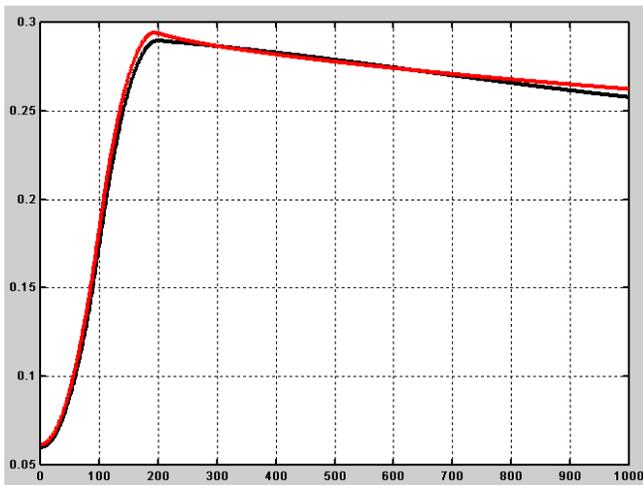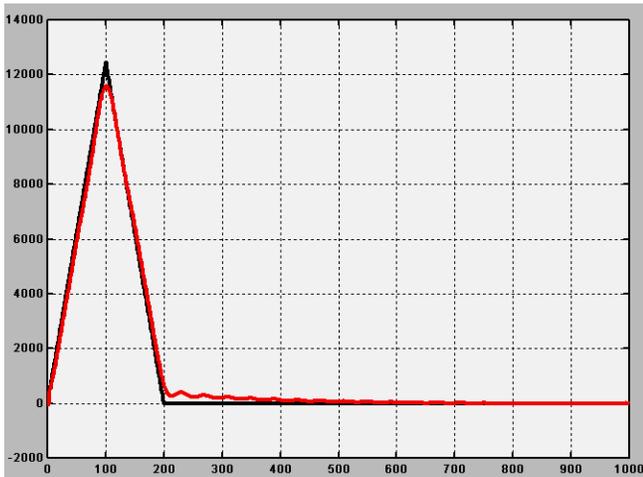(*a*) u_{mean}, m/s

(*b*) *P*, Pa

Figure 5 CFD (*Fluent*, black) and *Mathematica* analytical (red) calculations for (*a*) mean velocity and (*b*) pressure profiles for triangular pulse profile described in the text.

Fluent simulations were performed over one cycle with a time-step of 0.001 s. The version of the code used required the velocity profile to be provided as input, so this was supplied from the analytical solutions. Data for comparison were taken at a position 0.5 m from the entrance in order to eliminate entry effects which were evident up to 0.2 m. The agreement between calculated and simulated average velocities in Figure 5(*a*) is good. The pressure gradient calculated using Fluent and that provided to the analytical approaches are compared in Figure 5(*b*) and again the agreement is excellent; the small oscillations just after t_1 are due to the errors in evaluation and numerical integration of the higher frequency terms in the Fourier series. It should be noted that the *Mathematica*™ solutions were obtained

within minutes, whereas the *Fluent* code required hours of CPU time. The reliability and speed of the analytical approaches was therefore considered good.

Shear stress enhancement

The increase in shear stress caused by flow pulsing is here reported as a ratio, τ^*, defined as

$$\tau^* = \frac{\tau_w(P')}{\tau_w(P_{ss}')}$$ [16]

and results are presented for a pulse with characteristics P'_p = -1250 Pa/m, P'_{ss} = -50 Pa/m, t_1 = 0.2, t_2 = 0.5 s. The Green function approach is used unless otherwise stated. Figure 6 shows the shear stress enhancement for both geometries under these conditions, with both cases exhibiting a 7-8 fold increase in shear stress which lags the pressure pulse.
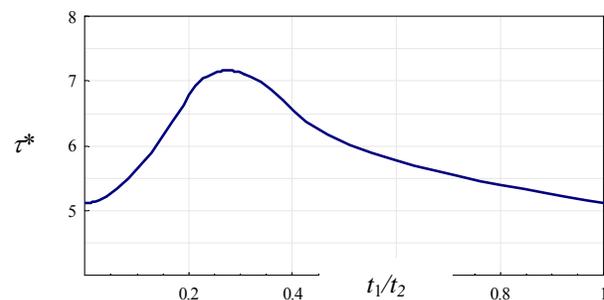
(*a*)
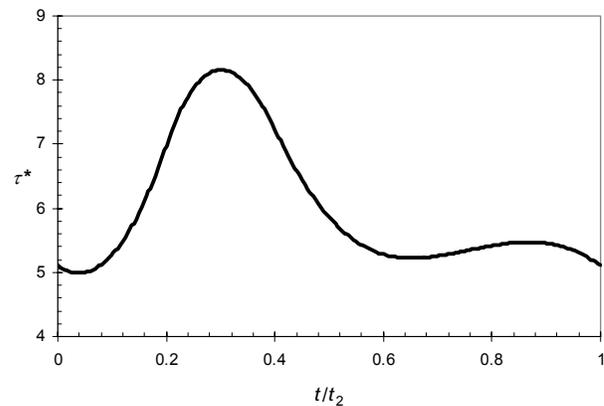
(*b*)

Figure 6 Ratio of wall shear stresses for (*a*) tube flow and (*b*) inner surface of annulus.

The secondary peak evident in Figure 6(*a*) at $t/t_2 \sim 0.8$ is suspect and requires further investigation in order to

eliminate numerical error as a source of this feature. An interesting feature of the profiles is that τ^* never relaxes to unity over this time period, suggesting that an intermittent pulse can increase the shear stress at the wall over the whole period, with implications for pumping costs as well as less fluid needing to be pumped in order to give the same increase in shear stress.

The enhancement in wall shear stress will ultimately depend on the form of the pressure gradient: the approaches described here can be applied to a wide range of forms (see Patel and Pore (2003) and Celnik (2004)). Figure 7 shows how the amplitude and periodicity of the intermittent triangular pulse shown in Figure 2 affect the shear stress at the inner wall of an annulus. The triangular pulse results in a significant improvement in shear, such that it can readily be doubled with the flow still in the laminar regime. Extending the prediction beyond the laminar threshold is non-trivial as the generation of eddies in the transition regime is not covered by the solutions.
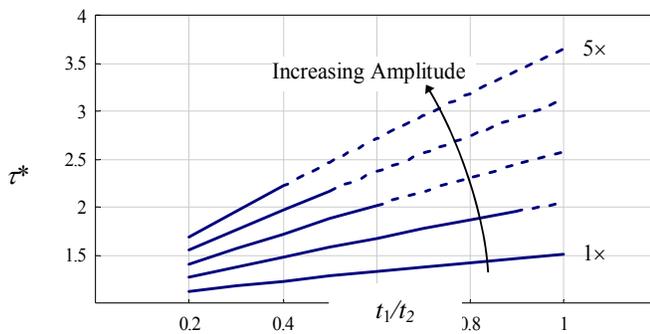

Figure 7 Improvement to shear stress on annulus inner wall for intermittent tri-pulse pressure gradient. Conditions: P'_{ss} = -50 Pa/m and lines of increasing amplitude show $P'_p = m \times P'_{ss}$. Dashed lines indicate combinations where Re_{max} exceeds the laminar regime limit of 2000.

Equivalent flow comparison

The above comparisons have used the steady term pressure gradient, and therefore steady flow mean velocity, as a reference but an alternative basis for comparison would be to compare the profiles on the basis of equivalent flow rate, *i.e.* the same volume of liquid is used, or the steady flow which corresponded to the average of the flow over the intermittent pulse cycle. Figure 8 shows the shear stress enhancement data from Figure 7 re-plotted using this criterion and a noticeably smaller improvement over the equivalent steady flow case is apparent. A noticeable difference arises in that the improvement decreases as the triangular pulse length, t_1, increases.
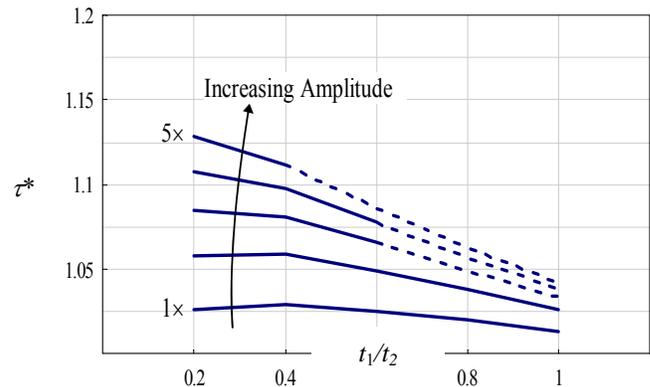

Figure 8 Improvement in shear stress on annulus inner wall for an intermittent triangular pulse for the equivalent steady flow case. Dotted lines indicate that the system is no longer in the laminar regime. P'_{ss} = -50 Pa/m: P'_p shown as multiples thereof.

These examples illustrate the scope of the approach, which offers significant advantages over CFD in calculating potential wall shear stress enhancement in viscous or slow flows.

CONCLUSIONS

An analytical approach to quantifying the enhancement of wall shear stress offered by intermittent flow pulsing, based on pressure gradient data, has been developed for the tubular and annular flow geometries, commonly used in fouling and cleaning studies. The results obtained in relatively short periods of computation time were consistent with previously published solutions and CFD simulations. The solutions are strictly only valid in the laminar regime and a noteworthy observation is that the conditions employed by Gillham and co-workers to enhance the cleaning of whey protein deposits were likely to have promoted turbulence in their system.

One area for future work is to identify the threshold of laminar behaviour under these transient conditions.

ACKNOWLEDGEMENTS

NOMENCLATURE

a	annulus inner radius, m
a_j, b_j	coefficients in Fourier series
b	annulus outer radius, m
ber, *bei*	Kelvin functions
G, G_{vel}	Green function, velocity
i	$\sqrt{-1}$
J_n	Bessel function of first kind, n^{th} order
L	operator
m	arbitrary constant
N	number of terms in Fourier series
P	pressure, Pa
P'	pressure gradient, Pa/m
r	radial co-ordinate, m
R	tube radius
Re	Reynolds number
S	track length, m
t	time, s
t_1	length of triangular pulse, s
t_2	total length of periodic pulse, s
u	axial velocity, m/s
x	arbitrary variable
z	axial co-ordinate, m
β	dimensionless radius, r/R
δ	Dirac delta function
λ	root defined by Equation [7]
Λ	root, see Equation [14]
μ	viscosity, Pa s
ρ	density, kg/m³
τ^*	ratio of enhanced to steady shear stress
τ_w	wall shear stress, Pa
ω	frequency of periodic pulse, $= 2\pi/t_2$, s⁻¹

Subscript

cos	term defined by Equation [5]
max	maximum value
p	pulsation
sin	term defined by Equation [6]
ss	steady flow
vel	velocity
n,j	indices in series

REFERENCES

M. Abramowitz and I.A. Stegun, 1967, *Handbook of Mathematical Functions with Formulas, Graphs and Mathematical Tables*, US Dept. of Commerce, Applied Maths Series # 55.

W. Augustin and M. Bohnet, 1999, Influence of pulsating flow on fouling behaviour, Proceedings of the Engineering Foundation Conference on Mitigation of Heat Exchanger Fouling and its Economic and Environmental Implications, Banff, Canada.

W. Augustin and M. Bohnet, 2001, Einfluss einer pulsierenden Stroemung auf das Foulingverhalten an warmeubertragenden Flachen, *Chem. Ing. Tech.*, Vol. 73(9), pp. 1138-1144.

G.K. Batchelor, 1979, *An Introduction to Fluid Mechanics,* Cambridge University Press, Cambridge, UK.

K. Bode, R.J. Hooper, W. Augustin, S. Scholl, W.R. Paterson and D.I. Wilson, 2005, Pulsed flow cleaning of whey protein fouling layers, this meeting.

M.Ö Çarpinlioğlu and M.Y. Gündoğdu, 2001, A critical review on pulsatile pipe flow studies directed towards future research topics, *Flow Measurement Inst.*, Vol. 12, pp. 163-174.

M.Ö Çarpinlioğlu, 2003, An approach for transition correlation of laminar pulsatile pipe flows via frictional field characteristics, *Flow Meas. Instr.*, Vol. 14, 233-242.

M.S. Celnik, 2004, Pulsed flow cleaning in an annulus, MEng Project Report, Department of Chemical Engineering, University of Cambridge.

M.S. Celnik, M.J. Patel, M. Pore, D.M. Scott and D.I. Wilson, 2005, Calculation of velocity profiles and wall shear stresses in pulsed laminar duct flows, *Chem. Eng. Sci.* (submitted).

J.Y.M. Chew, V. Höfling, W. Augustin, W.R. Paterson and D.I. Wilson, 2005, A method for measuring the strength of scale deposits on heat transfer surfaces. *Dev. Chem. Engng. Min. Proc.*, Vol. 13(1/2), 21.

F.M. Donovan, R.W. McIlwain, D.H. Mittmann and B.C. Taylor, 1994, Experimental correlations to predict fluid resistance for simple pulsatile laminar flow of incompressible fluids in rigid tubes, *Trans ASME J Fluids Eng.*, Vol. 116, pp516-521.

M.F. Edwards and W.L. Wilkinson, 1971, Review of potential applications of pulsating flow in pipes, *Trans. IChemE*, Vol. 49, pp. 85-93.

C.R. Gillham, 1997, Enhanced cleaning of surfaces fouled by whey protein, PhD dissertation, University of Cambridge.

C.R. Gillham, P.J. Fryer, A.P.M. Hasting, and D.I. Wilson, 2000, Enhanced cleaning of whey protein soils using pulsed flows, *J. Food Engng.*, Vol. 46, pp. 199-209.

 J. Harris, G. Peev and W.L. Wilkinson, 1969, Velocity profiles in laminar oscillatory flow in tubes, *J. Sci. Instr.*, Series 2, Vol. 2, pp. 913-916.

M.J. Patel and M. Pore, 2003, Modelling the enhancement of cleaning using pulsed flow, MEng Project Reports, Department of Chemical Engineering, University of Cambridge.

S. Uchida, 1956, The pulsating viscous flow superposed on the steady laminar motion of incompressible fluid in a circular pipe, *Zeitschrift fur Angewandte Mathematik und Physik*, Vol. 7, pp. 403-422.

W. M. Washington and C. L. Parkinson, 1986, *An introduction to three-dimensional climate modeling,* University Science, Mill Valley, California, USA.